IEEE Access
Multidisciplinary | Rapid Review | Open Access Journal

Received September 13, 2018, accepted October 7, 2018, date of publication October 16, 2018, date of current version November 9, 2018.

Digital Object Identifier 10.1109/ACCESS.2018.2876377

A Novel Patient-Specific Human Cardiovascular System Phantom (HCSP) for Reconstructions of Pulsatile Blood Hemodynamic Inside Abdominal Aortic Aneurysm

ANDRZEJ POLANCZYK[1,2], MICHAL PODGORSKI[3], MACIEJ POLANCZYK[2], ALEKSANDRA PIECHOTA-POLANCZYK[4], CHRISTOPH NEUMAYER[1], AND LUDOMIR STEFANCZYK[3]

[1]Faculty of Process and Environmental Engineering, Department of Heat and Mass Transfer, Lodz University of Technology, 90-924 Lodz, Poland
[2]Department of Surgery, Division of Vascular Surgery, Medical University of Vienna, 1090 Vienna, Austria
[3]Department of Radiology and Diagnostic Imaging, Medical University of Lodz, 90-647 Lodz, Poland
[4]Department of Medical Biotechnology, Faculty of Biochemistry, Biophysics and Biotechnology, Jagiellonian University, 31-007 Krakow, Poland

Corresponding author: Andrzej Polanczyk (andrzej.polanczyk@gmail.com)

The work was supported by the Polish National Centre for Research and Development under Grant 501/10-34-19-605 to AP.

ABSTRACT Background and objectives: Post-operative complications of endovascular aneurysm repair, such as endoleaks, migration, or angular bands in a stent-graft or narrowing and occlusion of a stent-graft lumen are potentially life-threatening and difficult to perceive without constant monitoring. Therefore, our work aimed to propose a new *ex-vivo* system called Human-Cardiovascular-System-Phantom (HCSP) to simulate pulsatile hemodynamic in the abdominal aortic aneurysm (AAA) before and after stent-graft placement. Materials and Methods: To verify the system twelve AAA-models, before and after medical treatment, were reconstructed based on medical data from AngioCT and US-Doppler. Furthermore, the 3D printed models were installed in the HCSP to reconstruct pulsatile flow and mechanical behavior of the aortic aneurysm wall which was tracked with DC. Clinical data, including results from 2D-Speckle-tracking-technique (2DSTT), were also used to verify wall deformation for heart rate ranging between 60 to 120 min^{-1}, and were confronted with results on wall deformation measured with DC in 3D printed aneurysms. Results: HCSP was able to track and calculate wall deformation with accuracy from 94.4% to 100% compared to 2DSTT. Wall deformation calculated with DC did not statistically vary from 2DSTT values. For instance, wall deformation measured with 2DSTT for anterior position and for 70 min^{-1} was equal to 4.18 ± 0.05 mm, 3.70 ± 0.08 mm and 2.00 ± 0.08 mm for AAA, AAA+thrombus and AAA+stent-graft, respectively. Those values were comparable with those measured with DC. Conclusions: The proposed HCSP allows to successfully follow hemodynamic changes in the AAA-model with thrombus or stent-graft and under different hemodynamic conditions. Thus, our approach may be useful in monitoring the influence of a stent-graft's spatial configuration on different hemodynamic parameters inside the AAA in the laboratory conditions.

INDEX TERMS Implants, stress control, stress measurement, structural shapes, surgical instruments, thrombosis, stent-graft, wall displacement.

I. INTRODUCTION

The number of patients with diagnosed abdominal aorta aneurysm (AAA) is still increasing [1]. Presence of thrombus inside an aneurysm may stiffen its wall and result in both: minimization of aneurysm wall pulsation or increase in the risk of aneurysm wall rupture. Therefore, endovascular methods (endovascular aneurysm repair; EVAR) are used to improve blood hemodynamic and minimize the risk of AAA rupture [2]–[4]. The EVAR methods are associated with lower postoperative complications compared to the open surgery interventions [5], [6]. Among the most important advantages of the EVAR methods are: no need

for laparotomy (surgical opening of the abdominal cavity), a reduction of intraoperative blood loss and a shorter recovery time [7], [8]. However, complications of the EVAR methods, such as endoleaks, migration or angular bands in the stent-graft [9]–[11] or more severe like stent-graft's lumen narrowing and occlusion may appear [12]–[15]. Additionally, thrombi can also develop inside the stent-graft, obstructing the blood flow. One of the methods used for investigation of blood flow through the vascular system are mathematical models [16]–[20]. This technique, supported with data from ultrasound and contrast enhanced computed tomography (AngioCT) is an attractive tool to reconstruct blood flow in different clinical conditions [21]–[23]. However, to further improve reliability of computational results, data from the Doppler ultrasound (US-Doppler), AngioCT, and magnetic resonance imaging (MRI) may be used to create the experimental devices for testing 3D models of the aorta (straight tube or printed models) [24]. This solution, gives the advantage of reconstructing blood flow through the different types and spatial configuration of vessels [21], [22]. Moreover, it gives the opportunity to test blood hemodynamic in different clinical conditions without exposing a patient to threat [25], [26]. Therefore, both *in vitro* and *ex vivo* research are performed to find new strategies to protect the circulatory system [27]–[29]. Nevertheless, as *in vivo* experiments may not directly reflect the changes in human body, *ex vivo* experiments have less limitations as they may be performed on tissues or on primary cells and may replicate hemodynamic factors that enable investigation of laminar and pulsatile flow under various pressure conditions [30]–[34]. However, most of the *ex vivo* models published so far deal with the laminar flow through the artificial arteries [35], [36] or graft preservation solutions [37]. Meanwhile, the pulsatile character of blood flow in the arterial system causes a strong and recurrent stretch of arteries' walls that may result in wall damage, especially in case of pre-existing alterations such as atherosclerosis [38]. Nonetheless, so far few efforts have been taken to exploit the potential of *ex vivo* vessel bioreactors towards a high-fidelity *ex vivo* replication of the hemodynamic factors affecting arterial wall behavior in an artificial environment [39]–[41]. Therefore, the aim of this study was to design a novel, patient-specific Human-Cardiovascular-System-Phantom (HCSP) for testing associations between spatial configuration of the AAA models and changes of blood hemodynamic as well as aortic wall deformations. This approach allows to analyze data from three groups of patients: with the AAA,;ith the AAA and artificial thrombus attached to the wall,;nd with the AAA after stent-graft placement.

In Section II experimental setup, medical data processing and preparation of the 3d elastic model of AAA, examination conditions and statistical analysis in the paper are described. Section III presents the results described in the mathematical description of aortic wall deformation with the use of HCSP system. In Section IV proposed system properties are discussed while Section V concludes the paper.

II. MATERIAL AND METHODS

A. PHANTOM CONSTRUCTION

In this study we designed and build Human-Cardiovascular-System-Phantom (HCSP) that is a phantom of cardiovascular system that allows reconstruction of blood hemodynamic in printed models of the aorta and/or AAA (Figure 1). The main part of the installation is a transparent, rectangular, container made of plexy (Figure 1D) (15 liters of capacity) where elastic 3d AAA models (Figure 1E) (described below) were placed. The pump (Figure 1F) was supplying the model with non-commercial fluid mimicking blood's rheological properties, which consisted of 60% of distilled water and 40% of glycerol (density of 1.2 g cm^{-3} and viscosity of 4.8×10^{-3} Pa·s) [24]. The pulsating character of a flow was achieved with the use of originally designed and build pulsator, placed on the top of the installation. A moving plager placed in a stainless-steel corpus called an artificial heart (Figure 1A) regulated ejection pressure, ejection volume, and frequency of pulsation. These parameters were controlled by an electrical engine connected to the computer. The pulsator was supplied with a self-constructed electric impulse generator to adjust entry values according to the ECG trace recorded each time in analyzed patients (described below) [42]. Different ECG records, obtained from the analyzed patients, were set each time as an inlet boundary condition for our phantom for specific 3d model of AAA. Therefore, each time, a specified amount of medium supplies the analyzed vessel. Moreover, hemodynamic parameters, e.g., flow/velocity and pressure were monitored with the use of ultrasound flow meters (Figure 1B) and pressure sensors (Figure 1C). To set realistic inlet conditions at the

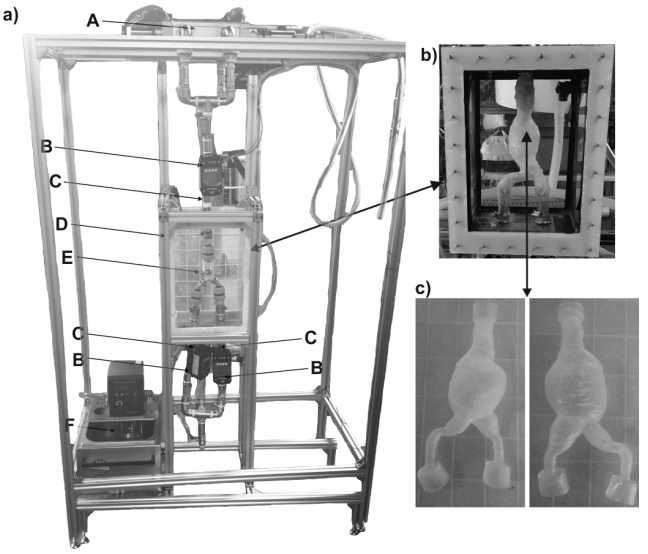

FIGURE 1. Human Cardiovascular System Phantom (HCSP) for reconstructions of pulsatile blood hemodynamic: a) an installation for reconstruction of pulsatile blood hemodynamic: A - a pulsator, B - flow sensors, C - pressure sensors, D - a transparent rectangular container, E - an example of 3d model of abdominal aortic aneurysm, F - a pump; b) a transparent rectangular container; c) an example of abdominal aortic aneurysm 3d model (front and back view).

inlet of analyzed vessels, the artificial heart was designed and programmed. It mimicked the blood hemodynamic as we previously described [43]. Moreover, technical specification of applied sensors included: 0.024–60 L/min ±2% (ultrasound flow meters, made by Bamo), 0–6 bar ±0.5% (pressure sensor, made by Wika). Furthermore, to simulate the internal pressure that exists within the abdominal cavity, the vessel chamber was filled with non-commercial fluid mimicking blood's rheological properties. Liquid was directed through the AAA models fixed in the container.

Supervisory control and data acquisition (SCADA) system for the measurement of pressure, flow and velocity in real time, was prepared with the use of LabView 2011 software (National Instrument, USA). The SCADA system controlled pulsatile flow through the invertors connected with the pump and pulsator. Pulsation of the AAA wall was measured in two ways: (i) with the ultrasound 2D-Speckle tracking technique (2DSTT) (GE Vivid 7, GE Healthcare, USA) and (ii) with the use of digital camera (DC) system.

One set of 10 cycles of systole and diastole pressure was recorded for three sides: anterior, posterior and lateral. Due to the shape of the AAA that was curved in most cases, the AAA wall that was most distant from the container's wall was not evaluated. Examinations were performed for each side separately to clearly visualize the closest segment of the AAA wall. The AAA models were examined in three clinical groups: (i) the AAA without the thrombus and stent-graft (AAA), (ii) the AAA with the thrombus at the posterior wall (AAA+thrombus), and (iii) the AAA after implantation of the stent-graft (AAA+stent-graft) (Zenith; COOK; Cook Medical, USA). Models without thrombus or stent-graft were used as a reference to evaluate the influence of both these elements on blood hemodynamic. Both, stent-grafts and thrombus were placed in the same position as in the analyzed patients.

B. MEDICAL DATA PROCESSING AND PREPARATION OF THE 3D ELASTIC MODEL OF AAA

We used AngioCT data (GE Light-Speed 64 VCT; GE Healthcare, Fairfield, CT, USA) for the reconstruction of twelve digital aneurysm geometries, further utilized to create an elastic 3d models of AAA. We analyzed three groups of male patients: (i) AAA (n=4), (ii) AAA+thrombus (n=4) (iii) AAA+stent-graft (n=4). Patients with stent-grafts were examined before and after stent-graft placement. Patients clinical description was gathered in Figure 2 and thoroughly described in our previous paper [42]. Patients' data were retrospectively collected after obtaining written informed consent to participate in the study. Medical data and images were anonymized by coding information before access and analysis. The study protocol was approved by the local ethics committee of Medical University of Lodz (RNN/126/07/KE).

Average inlet and outlet diameters (left and right) for the AAA and AAA+stent-graft groups were approximately 23.86±0.85 mm, 19.05±0.33 mm, and 18.98±0.29 mm. Whereas, for the AAA+thrombus group average inlet and outlet diameters were 23.75±1.04 mm, 19.25±0.31 mm, and 19.28±0.29 mm. Moreover, the average aneurysm diameter for all patients was approximately 86.13±6.91 mm (90.00±6.78 mm, 80.38±3.59 mm and 88.00±6.88 mm for the AAA, AAA+stent-graft and AAA+thrombus, respectively).

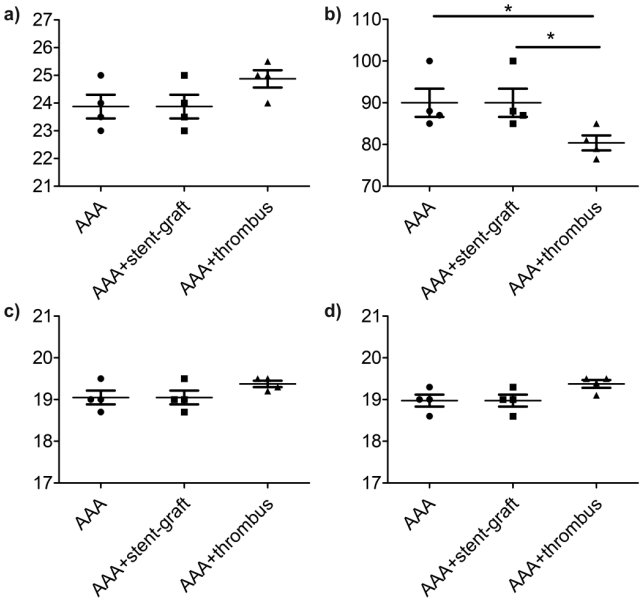

FIGURE 2. Clinical description and geometric characteristics of investigated Abdominal Aortic Aneurysms. a) inlet diameter measured in millimeters; b) aneurysm sac diameter measured in millimeters; c) left outlet diameter measured in millimeters; d) right outlet diameter measured in millimeters. AAA – patients with aneurysm without stent-graft and thrombus inside; AAA+stent-graft – patients with stent-graft; AAA+thrombus – patients with thrombus inside.

To prepare a virtual 3d geometries of the AAA models we used the 3DDoctor software (Able Software Corp., Lexington, MA, USA) which utilizes medical data [44]. We based on data from medical imaging technique, AngioCT, which visualized arteries just below the renal arteries and up to both iliac arteries which allowed us to evaluate the morphology of the abdominal aortic aneurysm. The resolution of medical data is of importance and we used 512 × 512 and approximately 600 slices with voxel size of 0.44 mm × 0.44 mm × 0.63 mm. At the first step, AngioCT data had to be manually adjusted for brightness to achieve the highest contrast between blood vessels and surrounding tissues. Then, the region growing technique was applied to extract vessels from the background. Next, due to large brightness intensity variation inside the vessel, we used ImageJ software (Wayne-Rasband, NIH) for manual filling of small gaps inside the blood vessel's wall. Finally, 3DDoctor software was applied to build 3D virtual models of analyzed vessels, which were eventually printed with the use of 3D printing technique. In each case the inlet to the model was just below the superior mesenteric artery origin and the outlets were localized in the common iliac arteries at the level below the stent-graft ending. Next, the 3d AAA models were

printed from an elastic material Tango Plus (tensile strength 0.8-1.5 MPa, elongation at break 170-220%, compressive set 4-5%, shore hardness 26-28 scale A, tensile tear resistance 2-4 kg cm^{-1}, polymerized density 1.12-1.13 g cm^{-3}), which resembles biomechanical features of the arterial wall (3D printer, Object Eden 350, USA). Artificial thrombus was made of the same material as the AAA models and was located each time in the lumen of the aneurysm after making two-centimeter-long incision at the superior aspect of the posterior wall. Next, the thrombus was fixed with silicon to the posterior wall, close to the line of incision. The incision was also closed with the silicon. Each time the shape of the thrombus was reconstructed from AngioCT data of a specific patient. Similarly, stent-graft placement was alike the thrombus location. A stent-graft was fixed to the wall of the aneurysm with standard hooks *via* an incision which was closed with silicone. All records of wall movement were recorded at least four centimeters from the lines of incisions to avoid incorrect measurements.

C. EXAMINATION CONDITIONS

Each model was tested for four hemodynamic conditions (heart rate and left ventricle stroke volume). First, under conditions recorded from patients at a day of ultrasound strain examination. Next, two higher and one lower hemodynamic condition comparable to the one observed in a clinic were tested. Therefore, for each patient four hemodynamic conditions were checked (Table I).

TABLE 1. Hemodynamic parameters for analyzed patients.

Analyzed hemodynamic	Frequency of pulsation [min^{-1}]	Ejection volume [ml]
Clinical conditions	70	
Artificial conditions	60 90 120	70

Moreover, for each analyzed patient wall deformation was measured during ten contraction-relaxation cycles with the use of 2D-Speckle tracking technique (2DSTT) and GE Vivid 7 ultrasound apparatus (GE Medical System, Milwaukee, WI, USA) with a high-resolution linear transducer (14 MHz). The same procedure was repeated for 3d AAA models. This allowed to verify matching of experimental setting and AAA models with clinical data. Moreover, data form 2DSTT were compared with data of wall deformation recorded with digital camera (DC) connected to the installation.

D. STATISTICAL ANALYSIS

Statistical analysis was performed using Statistica12.0 (Tulsa, USA). Data were presented as mean±SD (standard deviation). In statistical analysis $p<0.05$ was considered significant. Normality of data distribution was checked with the Shapiro-Wilk test. Analysis of variance with the post-hoc tests (Turkey test) was used to evaluate differences in strain parameters for each wall segment with different fluid pressures applied. The Friedman analysis of variance for repeated measurements with dedicated post-hoc tests was used to evaluate differences in strain parameters for each wall segment between different fluid pressures and different clinical conditions.

III. RESULTS

The HCSP associated with 2DSTT and DC allowed to reconstruct wall deformation of twelve artificial aneurysm models which were compared to clinical data calculated with 2DSTT. We also analyzed wall deformation for lower and higher frequency of heart rate using 2DSTT and DC.

Firstly, clinical data were used to verify wall deformation for the heart rate of 70 min^{-1}. Those results were next confronted with wall deformation obtained for artificial aneurysms measured with DC and 2DSTT (Figure 3). As the shape of aneurysms was not uniform, we analyzed anterior, lateral and posterior wall separately. For clinical data wall deformation for anterior position was equal to 4.23±0.10 mm, 3.85±0.13 mm and 2.05±0.21 mm for AAA, AAA+thrombus and AAA+stent-graft, respectively (Figure 3a), which was comparable with wall deformation of artificial aneurysms measured with 2DSTT and DC. The accuracy of wall deformation measurements recorded with the 2DSTT and DC compared to clinical data reached 98.8% and 99.4% for AAA, 96.1% and 98.1% for AAA+thrombus (Figure 3b) and, 97.6% and 97.6% for AAA+stent-graft (Figure 3c).

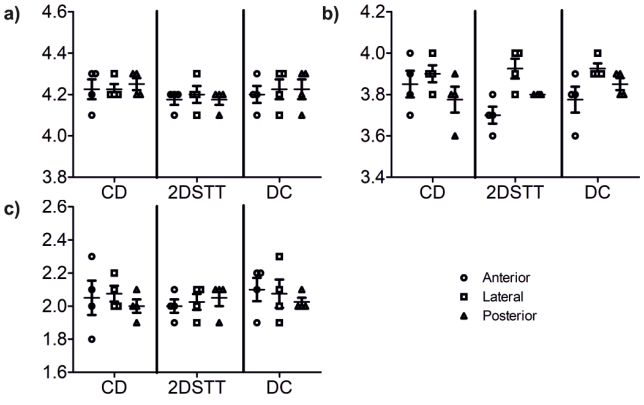

FIGURE 3. Values of wall deformation measured in millimeters acquired from clinical and experimental data for the 70 min^{-1} heart rate. a) AAA patients b) AAA+thrombus c) AAA+stent-graft. Values are presented as mean±SD. 2DSTT - 2D-Speckle tracking technique, DC- digital camera N=4 in each case. CD – clinical data.

In case of lateral position wall deformation for clinical data was equal to 4.23±0.05 mm, 3.90±0.08 mm and 2.08±0.10 mm for AAA, AAA+thrombus and AAA+stent-graft, respectively (Figure 3a). This was comparable with data gathered for artificial aneurysms calculated with the 2DSTT and DC. Similarly, like for anterior position the accuracy of experimentally calculated wall deformation for AAA, AAA+thrombus and AAA+stent-graft was respectively: 99.4%, 99.4% and 97.6% for the 2DSTT

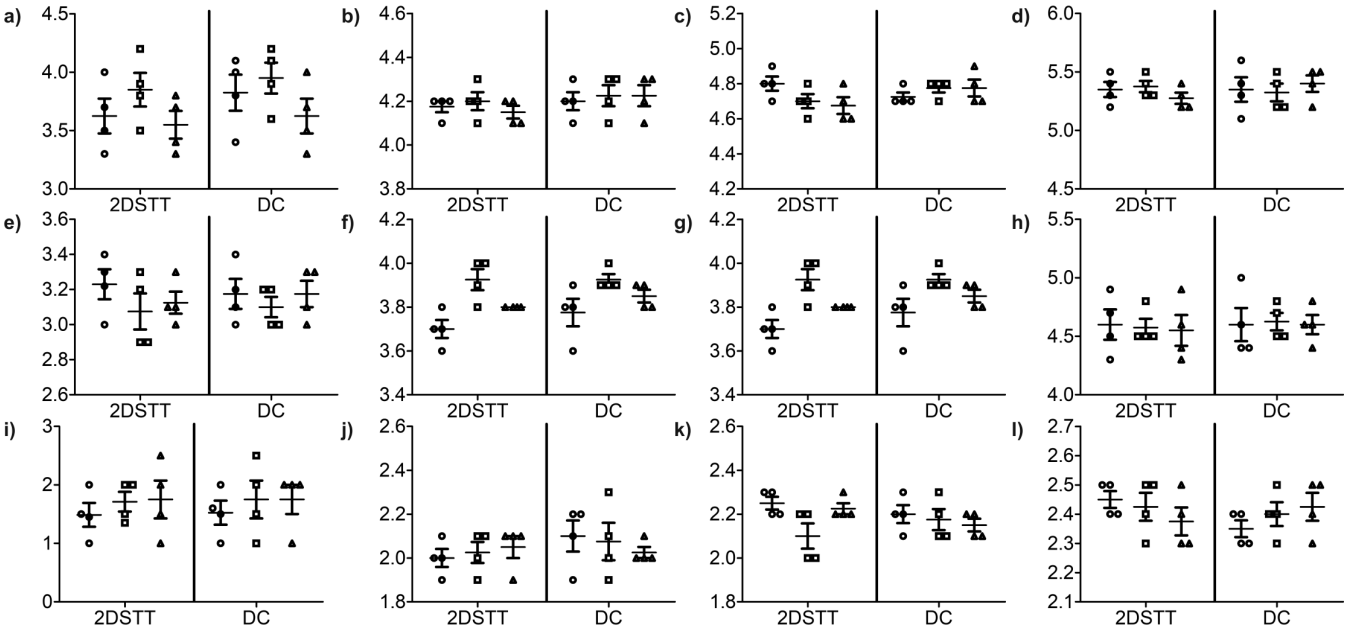

FIGURE 4. Values of wall deformation acquired experimentally with 2DSTT and digital camera selected heart rates heart rates. a) AAA - 60 min^{-1}, b) AAA - 70 min^{-1}, c) AAA - 90 min^{-1}, d) AAA - 120 min^{-1}, e) AAA+thrombus - 60 min^{-1}, f) AAA+thrombus - 70 min^{-1}, g) AAA+thrombus - 90 min^{-1}, h) AAA+thrombus - 120 min^{-1}, i) AAA+stent-graft - 60 min^{-1}, j) AAA+stent-graft - 70 min^{-1}, k) AAA+stent-graft - 90 min^{-1}, l) AAA+stent-graft - 120 min^{-1}, Values are presented as mean±SD. 2DSTT - 2D-Speckle tracking technique, DC- digital camera. N=4 in each case.

and 100%, 99.4% and 100% for the DC compared to the clinically estimated values. Finally, wall deformation in the posterior position for clinical data was equal to 4.25±0.06 mm, 3.78±0.13 mm and 2.05±0.10 mm for AAA, AAA+thrombus and AAA+stent-graft, respectively, which was comparable with artificial aneurysms 4.18±0.05 mm, 3.80±0.00 mm and 2.05±0.10 mm for the 2DSTT and 4.23±0.10mm, 3.85±0.06 mm and 2.03±0.05 mm for the DC.

Secondly, we analyzed wall deformation for wider range of heart rate (60 min^{-1}, 70 min^{-1}, 90 min^{-1} and 120 min^{-1}) for AAA, AAA+stent-graft and AAA+thrombus in anterior, lateral and posterior wall with the use of 2DSTT and DC (Figure 4). The results indicated that wall deformation values increased with increasing frequency of pulsation and that changes in wall deformation were smallest in case of AAA+stent-graft compared to AAA or AAA+thrombus.

Importantly, the results presented that in all analyzed cases the HCSP system was able to track and calculate wall deformation with accuracy from 94.4% to 100% compared to 2DSTT. The precision depended on aneurysm shape and wall position. Wall deformation calculated with the DC did not statistically vary from 2DSTT values. For instance, wall deformation measured with the 2DSTT for anterior position for 60 min^{-1} was equal to 3.62±0.30 mm, 3.23±0.17 mm and 1.49±0.41 mm for AAA, AAA+thrombus and AAA+stent-graft, respectively, which was comparable with 3.83±0.31 mm, 3.18±0.17 mm and 1.53±0.41 mm measured with the DC. Therefore, we accomplished 94.8%, 98.3% and 97.5% for AAA, AAA+thrombus and AAA+stent-graft, respectively compared to the DC. Whereas, for 70 min^{-1} wall deformations in the same plane was equal to 4.18±0.05 mm, 3.70±0.08 mm and 2.00±0.08 mm for AAA, AAA+thrombus and AAA+stent-graft, respectively which was comparable with values measured with the DC (Table IV). Similarly, wall deformation for anterior position for 90 min^{-1} was equal to 4.80±0.08 mm, 3.70±0.08 mm and 2.25±0.06 mm for AAA, AAA+thrombus and AAA+stent-graft, respectively, which was comparable with values measured with the DC (4.73±0.05 mm, 3.78±0.13 mm and 2.20±0.08 mm, respectively). Also, no significant difference was shown for heart rate of 120 min^{-1} in the 2DSTT and DC.

IV. DISCUSSION

In our study we designed a HCSP system phantom and verified its usability in the analysis of twelve artificial AAA models reconstructed from medical data. Our results indicated that artificial AAA models behave similarly to the AAAs observed in clinical cases. This approach for a new *ex-vivo* model verification was in line with other authors [24], [45]. For instance, Bihari *et al.* investigated silicon model of aneurysm perfused in a pulsatile artificial circulatory system. They observed strong correlation between *in-vitro* and *ex-vivo* results [45]. Similarly, Urbina *et al.* [24] who designed artificial system for blood hemodynamic reconstruction in healthy aortic arch and aortic arch with coarctation, observed comparable results (approximately 80% of similarity) for clinical cases and artificial aortic arch with coarctation. Although this model approach is widely accepted, there are

multiple techniques for measuring and analyzing models' parameters.

In our study we used 2DSTT and DC techniques to describe wall deformation of the artificial AAA models in different physiological and pathological conditions. Both, techniques indicated that stent-graft decreases wall deformation and confirmed that it stabilizes the AAA wall which might decrease the potential risk of aortic rupture. Moreover, lower stresses on the wall might lead to a decrease in the risk of stent-graft movement. The approach which we used to evaluate our phantom was previously used by other authors. For instance Fadel *et al.* [46] proofed that echocardiography is a useful tool for investigation of aortic aneurysms. Whereas, Satriano *et al.* [47] proposed a 3D image-based approach to compute aortic wall strain maps *in-vivo*. Similar, observation had Karatolios *et al.* [48] who used time-resolved three-dimensional ultrasonography coupled with speckle-tracking algorithms and finite element analysis for analysis of 8 patients . They indicated that healthy abdominal aortas presented reduction of mean strains and increased spatial heterogeneity and more pronounced temporal desynchrony as well as delayed systole compared to the abdominal aortic aneurysm cases [48]. Furthermore, Derwich *et al.* [49] noticed that with the use of 4D-US strain imaging system functional differences between young, old, and aneurysmal aorta can be described. Their results showed that age and sex have influence on circumferential strain, as the maximum local strain amplitude was significantly higher in the young compared with the old or aneurysmal aorta [49].

Finally, we showed that the presence of the thrombus or stent-graft decrease wall deformation. This is in line with, Metaxa *et al.* [50] who indicated that posterior thrombus deposition in AAA models is associated with significantly lower growth rate and lower posterior maximum wall stress compared with that of AAA models with anterior thrombus deposition and could potentially indicate a lower rupture risk. However, for the AAA+stent-graft model we showed that the construction of the stent-graft and its anchorage significantly minimized the influence of pulsation frequency. It was in line with Metaxa *et al.* [50] who indicated that the risk of aneurysm rupture corresponded with the unique geometry of every individual abdominal aortic aneurysm as well as the mechanical properties and the local strength of the degenerated aneurysmal wall . Similarly, observed Bihari *et al.* who investigated silicon model of abdominal aortic aneurysm in a pulsatile artificial circulatory system. The authors presented that displacement parameters measured *in-vitro* by 3D ultrasound and laser scan micrometer or video analysis were significantly correlated with each other at pulse pressures between 40 and 80 mmHg. They also identified strong local differences in displacement and strain [45]. On the other hand, Li *et al.* [51] documented that stent-graft implantation significantly decreased blood pressure in an aneurysm sac and decrease pulsations on the aortic wall. Furthermore, Cheng *et al.* [22] presented that stent-graft implantation to thoracic aorta increase blood resistance from 21.0 N to 24.8 N. This increase may lower the risk of postoperative stent-graft complications such as stent-graft migration.

Therefore, the proposed patient-based phantom and the applied technique may become a useful tool for optimization of endovascular prosthesis implantation in laboratory conditions.

LIMITATION TO THE STUDY

However, we may see some limitations of the HCSP system. Firstly, we analyzed arteries which length was not longer than 30 cm, as well as the diameter of aneurysm not higher than 10 cm. Such size was dictated by the size of transparent container, where artificial vessel was positioned. Therefore, further adjustments of the vessel's container tank and test on shorter and longer arteries must be made to test its versatility. Secondly, the construction of inlet and outlet stub pipes is limited to the aorta and abdominal aortic aneurysm. Therefore, further adjustments should be made for smaller vessels like carotid arteries or veins.

V. CONCLUSIONS

The application of HCSP enabled to reconstruct blood hemodynamic for different physiological and pathological conditions of the AAA. Comparison of three groups of patients showed that the AAA+thrombus and AAA+stent-graft is characterized by lower wall pulsation comparing to the AAA model.

The implantation of the stent-graft and its anchorage significantly minimize the influence of frequency of pulsation. However, further studies are planned to determine parameters that may influence the process of optimization of spatial configuration of endovascular prosthesis.

REFERENCES

[1] A. Polańczyk, M. Podyma, L. Stefańczyk, and I. Zbiciński, "Effects of stent-graft geometry and blood hematocrit on hemodynamic in Abdominal Aortic Aneurysm.," *Chem. Process Eng.*, vol. 33, no. 1, pp. 53–61, 2012.

[2] R. M. Greenhalgh, L. C. Brown, G. P. Kwong, J. T. Powell, and S. G. Thompson, "Comparison of endovascular aneurysm repair with open repair in patients with abdominal aortic aneurysm (EVAR trial 1), 30-day operative mortality results: Randomised controlled trial," *Lancet*, vol. 364, pp. 843–848, Sep. 2004.

[3] R. M. Greenhalgh and J. T. Powell, "Endovascular repair of abdominal aortic aneurysm," *New England J. Med.*, vol. 358, pp. 494–501, Jan. 2008.

[4] C. K. Chong, T. V. How, and P. L. Harris, "Flow visualization in a model of a bifurcated stent-graft," *J. Endovascular Therapy*, vol. 12, pp. 435–445, Aug. 2005.

[5] J. S. Coselli and S. Y. Green, "A brief history of aortic surgery: Insight into distal aortic repair," *J. Thoracic Cardiovascular Surg.*, vol. 145, pp. S123–S125, Mar. 2013.

[6] A. Polanczyk, A. Piechota-Polanczyk, and L. Stefańczyk, "A new approach for the pre-clinical optimization of a spatial configuration of bifurcated endovascular prosthesis placed in abdominal aortic aneurysms," *PLoS ONE*, vol. 12, p. e0182717, Aug. 2017.

[7] M. Lachat *et al.*, "Acute traumatic aortic rupture: Early stent-graft repair," *Eur. J. Cardio-Thoracic Surg.*, vol. 21, pp. 959–963, Jun. 2002.

[8] H. Ince and C. A. Nienaber, "The concept of interventional therapy in acute aortic syndrome," *J. Cardiac Surg.*, vol. 17, pp. 135–142, May 2002.

[9] C. L. Hayter, S. R. Bradshaw, R. J. Allen, M. Guduguntla, and D. T. A. Hardman, "Follow-up costs increase the cost disparity between endovascular and open abdominal aortic aneurysm repair," *J. Vascular Surg.*, vol. 42, pp. 912–918, Nov. 2005.

[10] M. R. Go, J. E. Barbato, R. Y. Rhee, and M. S. Makaroun, "What is the clinical utility of a 6-month computed tomography in the follow-up of endovascular aneurysm repair patients?" *J. Vascular Surg.*, vol. 47, pp. 1181–1187, Jun. 2008.
[11] F. Cochennec, J. P. Becquemin, P. Desgranges, E. Allaire, H. Kobeiter, and F. Roudot-Thoraval, "Limb graft occlusion following EVAR: Clinical pattern, outcomes and predictive factors of occurrence," *Eur. J. Vascular Endovascular Surg.*, vol. 34, pp. 59–65, Jul. 2007.
[12] N. Demanget *et al.*, "Computational comparison of the bending behavior of aortic stent-grafts," *J. Mech. Behav. Biomed. Mater.*, vol. 5, pp. 272–282, Jan. 2012.
[13] G. Maleux, M. Koolen, S. Heye, B. Heremans, and A. Nevelsteen, "Mural thrombotic deposits in abdominal aortic endografts are common and do not require additional treatment at short-term and midterm follow-up," *J. Vascular Interventional Radiol.*, vol. 19, pp. 62–1558, Nov. 2008.
[14] M. Prinssen, E. Buskens, and J. D. Blankensteijn, "Quality of life after endovascular and open AAA repair. Results of a randomised trial," *Eur. J. Vascular Endovascular Surg.*, vol. 27, pp. 121–127, Feb. 2004.
[15] R. A. Baum, S. W. Stavropoulos, R. M. Fairman, and J. P. Carpenter, "Endoleaks after endovascular repair of abdominal aortic aneurysms," *J. Vascular Interventional Radiol.*, vol. 14, pp. 1111–1117, Sep. 2003.
[16] A. Polanczyk, M. Podyma, L. Stefanczyk, W. Szubert, and I. Zbicinski, "A 3D model of thrombus formation in a stent-graft after implantation in the abdominal aorta," *J. Biomech.*, vol. 48, pp. 425–431, Feb. 2015.
[17] A. Polanczyk, A. Piechota-Polanczyk, C. Domenig, J. Nanobachvili, I. Huk, and C. Neumayer, "Computational fluid dynamic accuracy in mimicking changes in blood hemodynamics in patients with acute type IIIb aortic dissection treated with TEVAR," *Appl. Sci.*, vol. 8, no. 8, p. 1309, 2018.
[18] A. Polanczyk *et al.*, "A novel method for describing biomechanical properties of the aortic wall based on the three-dimensional fluid-structure interaction model," *Interact. CardioVascular Thoracic Surg.*, 2018. doi: 10.1093/icvts/ivy252.
[19] A. Polańczy, T. Woźniak, M. Strzelecki, W. Szubert, and L. stefanczyk, "Evaluating an algorithm for 3D reconstruction of blood vessels for further simulations of hemodynamic in human artery branches," in *Proc. Signal Process., Algorithms, Archit., Arrangements, Appl. (SPA)*, vol. 5, Sep. 2016, pp. 103–107.
[20] Z. Yanru, W. Xiaoming, Y. Hengxin, and C. Lilin, "The human cardiovascular model with the baroreflex control of central nervous system," in *Proc. IEEE/ICME Int. Conf. Complex Med. Eng.*, vol. 2, May 2007, pp. 43–47.
[21] T. J. Gundert, A. L. Marsden, W. Yang, and J. F. LaDisa, "Optimization of cardiovascular stent design using computational fluid dynamics," *J. Biomech. Eng.*, vol. 134, p. 011002, Feb. 2012.
[22] S. W. K. Cheng, E. S. K. Lam, G. S. K. Fung, P. Ho, A. C. W. Ting, and K. W. Chow, "A computational fluid dynamic study of stent graft remodeling after endovascular repair of thoracic aortic dissections," *J. Vascular Surg.*, vol. 48, pp. 303–310, Aug. 2008.
[23] A. Polanczyk, M. Podgorski, T. Wozniak, L. Stefanczyk, and M. Strzelecki, "Computational fluid dynamics as an engineering tool for the reconstruction of hemodynamics after carotid artery stenosis operation: A case study," *Medicina*, vol. 54, no. 3, p. 42, 2018.
[24] J. Urbina *et al.*, "Realistic aortic phantom to study hemodynamics using MRI and cardiac catheterization in normal and aortic coarctation conditions," *J. Magn. Reson. Imag.*, vol. 44, pp. 683–697, Sep. 2016.
[25] H. Roos, M. Ghaffari, M. Falkenberg, V. Chernoray, A. Jeppsson, and H. Nilsson, "Displacement forces in iliac landing zones and stent graft interconnections in endovascular aortic repair: An experimental study," *Eur. J. Vascular Endovascular Surg.*, vol. 47, pp. 262–267, Mar. 2014.
[26] V. Deplano, Y. Knapp, L. Bailly, and E. Bertrand, "Flow of a blood analogue fluid in a compliant abdominal aortic aneurysm model: Experimental modelling," *J. Biomech.*, vol. 47, pp. 1262–1269, Apr. 2014.
[27] R. Mundargi *et al.*, "Novel sensor-enabled *ex vivo* bioreactor: A new approach towards physiological parameters and porcine artery viability," *BioMed Res. Int.*, pp. 1–8, Mar. 2015, doi: 10.1155/2015/958170.
[28] X. Yang *et al.*, "Wandering pattern sensing at S-band," *IEEE J. Biomed. Health Inform.*, pp. 1863–1870, Dec. 2017.
[29] X. Yang *et al.*, "S-band sensing-based motion assessment framework for cerebellar dysfunction patients," *IEEE Sensors J.*, p. 1, Aug. 2018.
[30] R. Sinha, S. Le Gac, N. Verdonschot, A. van den Berg, B. Koopman, and J. Rouwkema, "Endothelial cell alignment as a result of anisotropic strain and flow induced shear stress combinations," *Sci. Rep.*, vol. 6, Jul. 2016, Art. no. 29510.
[31] R. F. Kelly and H. M. Snow, "Characteristics of the response of the iliac artery to wall shear stress in the anaesthetized pig," *J. Physiol.*, vol. 582, pp. 731–743, Jul. 2007.
[32] M. Piola *et al.*, "Full mimicking of coronary hemodynamics for *ex-vivo* stimulation of human saphenous veins," *Ann. Biomed. Eng.*, vol. 45, pp. 884–897, Apr. 2017.
[33] M. Piola *et al.*, "A compact and automated *ex vivo* vessel culture system for the pulsatile pressure conditioning of human saphenous veins," *J. Tissue Eng. Regenerative Med.*, vol. 10, pp. E204–E215, Mar. 2016.
[34] F. Prandi *et al.*, "Alessandra, E. Penza, "Adventitial vessel growth and progenitor cells activation in an *ex vivo* culture system mimicking human saphenous vein wall strain after coronary artery bypass grafting," *PLoS ONE*, vol. 10, p. e0117409, Feb. 2015.
[35] D. Janke *et al.*, "The *'artificial artery'* as *in vitro* perfusion model," *PLoS ONE*, vol. 8, p. e57227, Mar. 2013.
[36] A. Thomas, H. D. Ou-Yang, L. Lowe-Krentz, V. R. Muzykantov, and Y. Liu, "Biomimetic channel modeling local vascular dynamics of pro-inflammatory endothelial changes," *Biomicrofluidics*, vol. 10, p. 014101, Jan. 2016.
[37] B. Winkler *et al.*, "Graft preservation solutions in cardiovascular surgery," *Interact. CardioVascular Thoracic Surg.*, vol. 23, pp. 300–309, Aug. 2016.
[38] C. W. Hicks, T. Obeid, I. Arhuidese, U. Qazi, and M. B. Malas, "Abdominal aortic aneurysm repair in octogenarians is associated with higher mortality compared with nonoctogenarians," *J. Vascular Surg.*, vol. 64, pp. 956..e1–965.e1, Oct. 2016.
[39] K. Krishnan *et al.*, "Ascending thoracic aortic aneurysm wall stress analysis using patient-specific finite element modeling of *in vivo* magnetic resonance imaging," *Interact. CardioVascular Thoracic Surg.*, vol. 21, pp. 471–480, Oct. 2015.
[40] R. Ascuitto, N. Ross-Ascuitto, M. Guillot, and C. Celestin, "Computational fluid dynamics characterization of pulsatile flow in central and Sano shunts connected to the pulmonary arteries: Importance of graft angulation on shear stress-induced, platelet-mediated thrombosis," *Interact. CardioVascular Thoracic Surg.*, vol. 25, pp. 414–421, Sep. 2017.
[41] T. Krüger, K. Veseli, H. Lausberg, L. Vöhringer, W. Schneider, and C. Schlensak, "Regional and directional compliance of the healthy aorta: An *ex vivo* study in a porcine model," *Interact. CardioVascular Thoracic Surg.*, vol. 23, pp. 104–111, Jul. 2016.
[42] A. Polanczyk, M. Podyma, L. Trebinski, J. Chrzastek, I. Zbicinski, and L. Stefanczyk, "A novel attempt to standardize results of CFD simulations basing on spatial configuration of aortic stent-grafts," *PLoS ONE*, vol. 11, p. e0153332, Apr. 2016.
[43] A. Polanczyk, M. Klinger, J. Nonobachvili, I. Huk, and C. Neumayer, "Artificial circulatory model for analysis of human and artificial vessels," *Appl. Sci.*, vol. 8, no. 7, p. 1017, 2018.
[44] A. Polańczyk, M. Strzelecki, T. Woźniak, W. Szubert, and L. Stefańczyk, "3D blood vessels reconstruction based on segmented CT data for further simulations of hemodynamic in human artery branches," *Found. Comput. Decis. Sci.*, vol. 42, pp. 359–371, Dec. 2017.
[45] P. Bihari *et al.*, "Strain measurement of abdominal aortic aneurysm with real-time 3D ultrasound speckle tracking," *Eur. J. Vascular Endovascular Surg.*, vol. 45, pp. 315–323, Apr. 2013.
[46] B. M. Fadel, H. Bakarman, M. Al-Admawi, O. Bech-Hanssen, and G. Di Salvo, "Pulse-wave Doppler interrogation of the abdominal aorta: A window to the left heart and vasculature," *Echocardiography*, vol. 31, pp. 543–547, Apr. 2014.
[47] A. Satriano, S. Rivolo, G. Martufi, E. A. Finol, and E. S. Di Martino, "*In vivo* strain assessment of the abdominal aortic aneurysm," *J. Biomech.*, vol. 48, pp. 354–360, Jan. 2015.
[48] K. Karatolios *et al.*, "Method for aortic wall strain measurement with three-dimensional ultrasound speckle tracking and fitted finite element analysis," *Ann. Thoracic Surg.*, vol. 96, pp. 1664–1671, Nov. 2013.
[49] W. Derwich *et al.*, "High resolution strain analysis comparing aorta and abdominal aortic aneurysm with real time three dimensional speckle tracking ultrasound," *Eur. J. Vascular Endovascular Surg.*, vol. 51, no. 2, pp. 187–193, Feb. 2016.
[50] E. Metaxa, N. Kontopodis, K. Tzirakis, C. V. Ioannou, and Y. Papaharilaou, "Effect of intraluminal thrombus asymmetrical deposition on abdominal aortic aneurysm growth rate," *J. Endovascular Therapy*, vol. 22, pp. 406–412, Jun. 2015.
[51] Z. Li, C. Kleinstreuer, and M. Farber, "Computational analysis of biomechanical contributors to possible endovascular graft failure," *Biomech. Model. Mechanobiol.*, vol. 4, pp. 221–234, Dec. 2005.

ANDRZEJ POLANCZYK received the Ph.D. degree in medical engineering in 2013. He is currently a Researcher and the Team Leader with the Lodz University of Technology, Poland, where he is also an Associate Professor with the Faculty of Process and Environmental Engineering. He participated in scientific grants in which he built the installation to simulate the blood flow through the abdominal section of the aorta. His research areas comprise biomedical, chemical and, environmental engineering. Recently, he received a Grant funded by The National Centre for Research and Development.

MICHAL PODGORSKI received the Ph.D. degree in radiology in 2016. He is currently a Researcher with the Medical University of Lodz, Poland, where he is also an Associate Professor with the Department of Radiology and Diagnostic Imaging. He has participated in scientific grants in which he investigated human cardiovascular system. His research areas are concentrated on radiology and medical image processing.

MACIEJ POLANCZYK received the Ph.D. degree in image processing in 2012. He is currently a Researcher with the Lodz University of Technology, Poland, where he is also an Associate Professor with the Faculty of Process and Environmental Engineering. He has participated in scientific grants in which he built the installation for visually impaired people. His research areas comprise biomedical and environmental engineering.

ALEKSANDRA PIECHOTA-POLANCZYK is currently an Associate Professor with the Department of Medical Biotechnology, Jagiellonian University, Krakow, Poland. Her research interests focus on finding of new anti-oxidative and anti-inflammatory proteins that could be potential markers and/or targets in treatment of cardiovascular diseases, as well as the role of Nrf2 and heme oxygenase 1 in cellular adaptation to oxidative stress and inflammatory reactions.

CHRISTOPH NEUMAYER is currently the Head of the Department of Vascular Surgery, Medical University of Vienna. His research areas are concentrated on the molecular mechanism of artery diseases and diabetes.

LUDOMIR STEFANCZYK is currently the Head of the 3rd Department of Radiology and Diagnostic Imaging, Medical University of Lodz. His research areas are concentrated on radiology and medical image processing.